Journal of Pharmaceutical and Biomedical Analysis 48 (2008) 814–821

Contents lists available at ScienceDirect

Journal of Pharmaceutical and Biomedical Analysis

journal homepage: www.elsevier.com/locate/jpba

Quantitative determination of diclofenac sodium in solid dosage forms by FT-Raman spectroscopy

Sylwester Mazurek, Roman Szostak*

Department of Chemistry, University of Wrocław, 14 F. Joliot-Curie, 50-383 Wrocław, Poland

ARTICLE INFO

Article history:
Received 28 February 2008
Received in revised form 5 August 2008
Accepted 6 August 2008
Available online 22 August 2008

Keywords:
Active ingredient quantification
FT-Raman spectroscopy
Diclofenac sodium
Neural networks
Chemometrics

ABSTRACT

The FT-Raman quantification of diclofenac sodium in tablets and capsules was performed with the help of the partial least squares (PLS), principal component regression (PCR) and counter-propagation artificial neural networks (CP-ANN) methods. For the analysed tablets, calibration models were built using unnormalised spectra and spectra normalised by the intensity of a selected band of an internal standard. Different pre-processing methods were applied for the capsules. To compare the predictive ability of the models, the relative standard errors of prediction (RSEP) were calculated. The 5 × 5 CP-ANN and PLS methods gave models of comparable quality, which were usually more efficient than the PCR ones. The RSEP error values for the tablets were in the range of 2.4–3.8% for the calibration and 2.6–3.5% for the validation data sets and for the three procedures applied. For capsules, the RSEP errors were in the range of 0.8–1.9% and 1.4–1.7% for the calibration and validation samples, respectively. Five commercial products containing 25, 50 or 75 mg of diclofenac sodium per tablet/capsule were quantified. Concentrations found from the Raman data analysis agree with the results of the reference analysis and correlate strongly with the declared values with the recovery of 99.5–101.3%, 99.7–102.0% and 99.9–101.2% for the PLS, PCR and CP-ANN methods, respectively. The proposed procedure can be a fast and convenient alternative to the standard pharmacopoeial methods of diclofenac sodium quantification in solid dosage forms.

1. Introduction

Diclofenac sodium, a sodium salt of 2-[(2,6-dichlorophenyl)aminophenyl]-acetic acid and a potent analgesic and anti-inflammatory agent, is commonly used in various drug formulations including tablets, capsules, drops, injections, suppositories, gels and ointments [1]. Several analytical methods for the quantification of this active pharmaceutical ingredient (API) have been developed. UV–vis spectroscopy [2–8], spectrofluorometry [9–11], liquid chromatography [12–20] and potentiometry [21–24] are the most well-known techniques. An application of Raman spectroscopy for the quantitative analysis of its injection solutions was also demonstrated [25].

A continuous increase of Raman spectroscopy applications as an analytical method for the quantification of complex mixtures, including pharmaceutical preparations, has been observed [26–29]. The technique, supported by chemometrics, enables the analysis of medicines often without any additional sample treatment, which can remarkably simplify and shorten the analysis. It is a particularly useful tool in the analysis of products with a high API content [30–36]. Nevertheless, Raman quantification of preparations with 2–5% API weights has been reported [25,37,38]. This is likely because aromatics APIs are usually much stronger Raman scatterers than excipients, which are typically aliphatic. In favourable cases it is even possible to perform a reliable quantitative analysis of an API content below a 0.1% (w/w) level with this method [39]. Moreover, Raman technique enables also quantification of pharmaceutical preparations when two or more solid-state forms of the constituents are present [40,41].

In the modelling of systems for which non-linear signal-answer dependencies are present, the advantage of neural networks over other chemometrics methods, such as partial least squares (PLS) and principal component regression (PCR), is well-known, and the number of their applications for spectral data analysis continues to grow systematically [42–48]. Nevertheless, networking techniques are mainly used as classification tools [49–52] and the application of this method for quantification problems is not very common [42,48].

Herein, we present the results of FT-Raman diclofenac sodium quantification in five commercial tablets and capsules obtained using the PLS, PCR and CP-ANN methods.

* Corresponding author. Tel.: +48 71 3757 238; fax: +48 71 3757 420.
E-mail address: rsz@wchuwr.pl (R. Szostak).

0731-7085/$ – see front matter © 2008 Elsevier B.V. All rights reserved.
doi:10.1016/j.jpba.2008.08.013

2. Experimental

2.1. Materials and sample preparation

The substances used, namely diclofenac sodium (Sigma–Aldrich), lactose (Pharma Cosmetic), microcystalline cellulose (Sigma–Aldrich), starch (POCH), magnesium stearate (Sigma–Aldrich), talc (Hasco-Lek), eudragit (Röhm Pharma), SiO_2 (POCH) and potassium ferrocyanide(II) trihydrate (POCH) were of pharmacopoeial purity [1,53] or of analytical grade. Four diclofenac sodium preparations in the form of tablets (A, B, C, D) or capsules (E), declared to contain 25–75 mg of API, were purchased in a local pharmacy.

Calibration and validation samples with the suitable weight ratios of compounds, randomly varied, were prepared by mixing pure, solid substances in a mortar for a few minutes to homogenise the powders. Approximately 200 mg of powder was used to prepare a pellet in a way similar to that adopted in IR spectroscopy. The commercial products were first ground and then processed further like the calibration samples. Only the content of the capsules was analysed. Additionally, in the case of the analysis of the tablets, an appropriate amount of $K_4[Fe(CN_6)]\cdot 3H_2O$, chosen as an internal standard, was added to each sample. New pellets were prepared as described above and Raman spectra were recorded again.

To check for the possible collinearity between the component's concentrations, concentration versus concentration graphs were plotted for the studied mixtures. No significant correlations were observed. The determination coefficients R^2 for these plots were in the 0.01–0.20 range.

2.2. Apparatus

A Nicolet Magna 860 FT-IR spectrometer interfaced with an FT-Raman accessory, with a CaF_2 beamsplitter and indium–gallium arsenide (InGaAs) detector, was used to carry out the measurements. The samples were placed in a rotating sample holder and illuminated by an Nd:YVO_4 laser line at 1.064 μm with a power of 350 mW at the sample without a converging lens; backscattered radiation was collected. Samples were rotated at a constant speed of approximately 200 rpm. The interferograms were averaged over 256 scans, Happ-Genzel apodised and Fourier transformed using a zero filling factor of 2 to give spectra in the 100–3700 cm^{-1} range at a resolution of 8 cm^{-1} for tablets and of 4 cm^{-1} for capsules.

UV–vis spectra were recorded using a Carry-5 Varian spectrometer.

2.3. Reference UV–vis analysis

Reference UV–vis analysis was performed according to a procedure described by Fabre et al. [2] and de Micalizzi et al. [5]. Six samples containing appropriate amounts of API mixed with the tablet mass were dissolved in a methanol–water mixture (1:1, v/v) giving solutions containing from 6.51 to 25.42 mg/L of diclofenac sodium. Using the first derivative of the UV–vis spectrum, a calibration curve (slope = 0.0260, intercept = 0.5453, R^2 = 0.9985) was constructed by the zero crossing technique (λ = 258 nm).

2.4. Computational methods

A sophisticated treatment of spectroscopic data is possible with a number of multivariate techniques. Undoubtedly the most common among them is the principal component analysis (PCA), which constitutes the first step of PCR and PLS analyses. However in the modelling of systems for which non-linear signal-answer dependencies are present, ANN seems to give better results. The FT-Raman quantification of diclofenac sodium was performed using PLS, PCR and CP-ANN methods.

2.5. Principal components regression

The principal components regression method generates the calibration model in two steps [54–57]. In the first one of these, the variables in the independent data matrix X, such as the Raman spectra of samples placed in columns, are transformed into new ones that are linear combinations of the original by principal component analysis. New variables are obtained in such a way that the variance they explain decreases from the first to the last, and that they are orthogonal. There are several ways of finding the principal components. A widely used technique for this is singular value decomposition (SVD). After PCA, the X data matrix is decomposed as follows:

$$X = SVD^T, \tag{1}$$

where the product of the S and V matrices is the T matrix of the principal components (factors or loadings), and D is the matrix of the coefficients (scores). In a second step, multiple regression is applied to the new variables and the measured Y property, which in this analysis is the components' concentrations, to obtain a matrix of regression coefficients B, according to:

$$Y = XB + E, \tag{2}$$

where E represents the error not accounted for by the model.

2.6. Partial least squares regression

The PLS method, developed by Wold [58], is the most commonly applied mathematical tool in the quantitative analysis of multivariate data. The method is used to establish a relationship between a set of dependent (response) variables, Y, and a set of predictor (independent) variables, X [54–62]. The procedure performs a principal component analysis on the independent variables matrix, while simultaneously maximising the correlation with the dependent variables matrix. The matrices X and Y are decomposed in the following way:

$$X = TP^T + E_X \tag{3}$$

and

$$Y = UQ^T + E_Y, \tag{4}$$

where T and U are loadings, and P and Q are score matrices.

2.7. Counter-propagation artificial neural networks (CP-ANN)

The architecture of a CP-ANN allows one to combine an unsupervised mapping technique, known as Kohonen mapping, with a supervised learning strategy [63–66]. The general concept of the CP-ANN used is shown in Fig. 1. A network is built up from two layers of neurons arranged in two-dimensional rectangular matrices, $N_x \times N_y$, where x and y are numbers of neurons in the x- and y-directions. The input (Kohonen) layer is supplied with input variables related to the considered objects, which, in our case is the number of diclofenac sodium mixtures. During the learning process, the target values (concentrations of the mixture ingredients) are given to the output layer, which has the same topological arrangement of neurons as the Kohonen layer. The algorithm selects the neuron with the weights closest to the input variables. The chosen vector is called the winning, excited or central neuron. Once the correction of the weights has been performed in the Kohonen layer, the position of the winning neuron is transferred from the input to

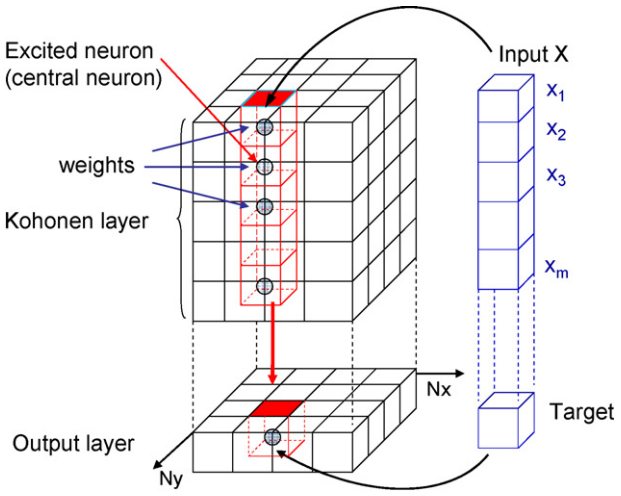

Fig. 1. General scheme of counter-propagation artificial neural networks (CP-ANNs) [63].

the output layer and the weights in the output layer are corrected according to the given target value. Step by step, by introducing one object after another, the weights in the Kohonen and output layers are corrected in such a way that they become more similar to the input variables. After the weights are stabilised, the CP-ANN is trained. However, the performance of the CP-ANN does not depend on the initiation of the weights, which is randomised.

In the prediction phase, the concentration values are picked up from the output layer. Following this stage, a new sample with an unknown compound concentration is presented to the system. It is first situated in the Kohonen layer, after which the position of the winning neuron is projected into the output layer and the result, such as concentration in our case, is extracted. The settings of the network parameters were adjusted to find optimal conditions for modelling purposes. For each system studied a test of network conditions, called screening, has to be carried out to find the lowest prediction error value for the validation data set.

2.8. Software and numerical data treatment

Nicolet TQ Analyst ver. 7 chemometrics software was used to construct the PLS and PCR models. CP-ANN computations were performed with the help of software developed by Zupan et al. from the Laboratory of Chemometrics, National Institute of Chemistry, Ljubljana (Slovenia) [64]. Numerical data were transformed into an appropriate format using the Matlab environment.

All spectral data were mean-centred. The quantitative composition of the studied samples was expressed as a mass fraction for models based on unnormalised spectra, or as a weight ratio for models constructed using spectra normalised by the maximum intensity or the integrated intensity of the ν_s(CN) potassium ferrocyanide band.

To characterise and compare the predictive abilities of the developed models, the relative standard errors of prediction, RSEP, were calculated according to the equation [67]:

$$\mathrm{RSEP}\,(\%) = \sqrt{\frac{\sum_{i=1}^{n}(C_i - C_i^{\mathrm{A}})^2}{\sum_{i=1}^{n}(C_i^{\mathrm{A}})^2}} \times 100, \tag{5}$$

in which C^{A} is the actual component content, C is the concentration found from Raman data analysis, and n is the number of samples. Direct comparison of various models based on data expressed in different concentration units, in our case the mass fraction and weight ratio, using the root mean square (RMS) error can sometimes be a cumbersome task. However, there is a simple relationship between the RSEP and RMS errors:

$$\mathrm{RSEP}\,(\%) = \sqrt{\frac{n}{\sum_{i-1}^{n}(C_i^{A})^2}}\,\mathrm{RMS} \times 100. \tag{6}$$

It is much more convenient to calculate RSEP errors, which are independent of the concentration units. In this text, we define the $\mathrm{RSEP_{cal}}$ parameter as the RSEP error for the calibration data set and $\mathrm{RSEP_{val}}$ for the validation one.

The predicted residual error sum of squares (PRESS) was calculated to select an optimal number of factors for the PLS models. The cross-validation technique (leave-one-out) was performed to estimate the robustness of the constructed models.

3. Results and discussion

In Fig. 2, the FT-Raman spectra of pure diclofenac sodium and of the studied commercial preparations are presented. All four analysed tablets, denoted A, B, C and D, contain the active component (17.0–23.2% by weight) in addition to starch, cellulose, magnesium stearate and silica in different proportions as excipients. Tablets A and C, and tablets B and D were produced by two different manufacturers. The composition of the tablet mass of preparations originating from the same manufacturer was similar.

3.1. Model construction and testing

To construct calibration models FT-Raman spectra of 29 solid samples, prepared as described above, were used. The mass fraction varied in the 0.08–0.34 range for diclofenac sodium, 0.09–0.42 for lactose, 0.09–0.33 for starch, 0.11–0.36 for cellulose and 0.04–0.16 for magnesium stearate. Six mixtures were chosen for the validation procedure and the validation data set was selected by the Kohonen mapping. The remaining 23 samples were used as a training set. This division between training and validation samples was preserved for all of the chemometrics models built (PLS, PCR and CP-ANN) including the internal standard approach.

The following spectral ranges were applied in the construction of the chemometrics models on basis of unnormalised spectra: 750.9–789.5, 1109.9–1209.2, 1270.0–1392.7, 1550.6–1635.4 and 2809.6–3092.9 $\mathrm{cm^{-1}}$. They do not include fragments of spectra with the lactose intense peaks, because lactose is not present in the B or D preparations. The listed regions were slightly modified for each

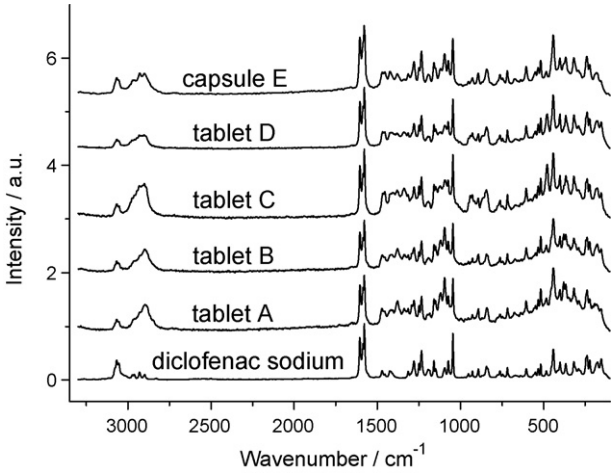

Fig. 2. FT-Raman spectra of diclofenac sodium and its analysed preparations.

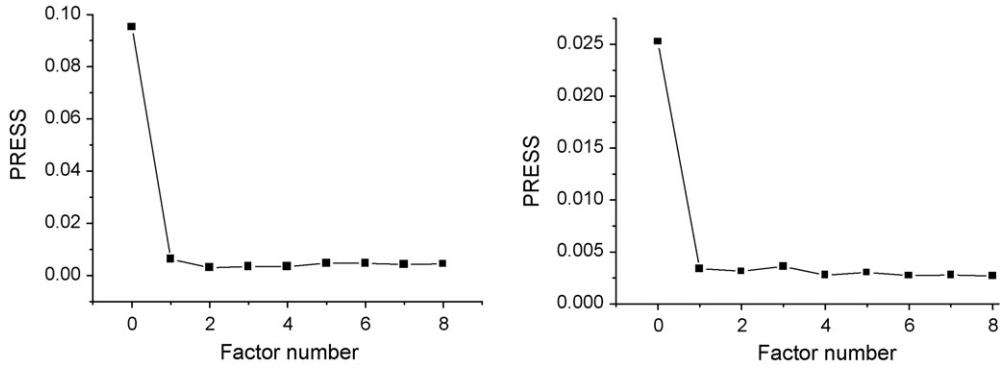

Fig. 3. PRESS values calculated for diclofenac sodium modelling in tablets (left) and in capsules (right).

preparation studied. From the PRESS plot for diclofenac sodium, presented in Fig. 3, it follows that it is enough to build the PLS model with the use of 3 factors.

The declared content of diclofenac sodium in preparation E amounts to 75 mg per capsule, which is 34.5% by weight. As the additives are different from those present in the studied tablets it was necessary to prepare a new calibration set; 35 mixtures containing the active substance, cellulose, eudragit, SiO_2 and talc were prepared in a way similar to that described above. The mass fraction varied in the range of 0.25–0.38, 0.25–0.37, 0.02–0.09, 0.24–0.35 and 0.02–0.05 for these constituents, respectively. The training set composed of 27 mixtures and a validation set including 8 samples were selected. Calibration models were constructed using the following spectral ranges: 699.1–939.2, 1060.7–1350.6, 1398.0–1460.9, 1552.9–1621.9 and 2802.2–3475.8 cm^{-1}. From the PRESS plot for diclofenac sodium (Fig. 3), one can see that 4 factors can be used for the PLS model construction.

3.1.1. CP-ANN modelling

Quantitative analysis using neural networking was also performed, and the results were correlated with those obtained from the PLS and PCR analyses. As one could expect, the selection of the spectral regions substantially influences the properties of the obtained models and the quality of the quantification of the unknown samples. In comparison to the PLS and PCR methods, the optimisation of neural networking seems to be more complex, because the number of possible network parameters influencing the strength of the model is usually larger.

The settings of the CP-ANN parameters were adjusted to find the optimal conditions for modelling by treating the set of n calibration samples, represented by Raman intensities at m selected wavenumbers, $m \approx 700$, as inputs. In our case n is equal to 23 or 27 for tablets or capsules, respectively. The predictive ability of the models depends noticeably on the network size, the number of neurons in the x- and y-directions ($N_x \times N_y$) and the number of learning epochs, which expresses the intensity of the network learning. During the screening procedure, the N_x (=N_y) values in the range of 3–7, namely the 9-, 16-, 25-, 36- and 49-neuron networks, were tested. The prediction ability of the network in the range of 25–500 learning epochs was screened, and, for some cases, we extended the number of cycles to 1000. The networks were trained using standard values of the maximal and the minimal correction factors settings, i.e. 0.5 and 0.01.

Fig. 4 shows the results of the screening procedure for the modelling of tablet A. The improvement of the $RSEP_{cal}$ parameter values with the elongation of the learning process is observed. The errors of prediction for the calibration set after 100 cycles are less than 2% in the case of $N_x = 6$ and 7 networks, while for the smallest CP-ANN ($N_x = 3$) their values are 4 times higher. Additionally, for smaller networks, the error values display periodical changes that are clearly visible for $N_x = 3$, 4 and 5 in the top map.

The plot of RSEP error values for the validation samples (Fig. 4) is more complex in comparison with the analogous plot for the training set. An initial decrease of the error values with the elongation of learning epochs is observed. Next, the minimum is reached. A further increase in the number of epochs does not result in improving the quality of the prediction, and errors often become higher. The lowest $RSEP_{val}$ errors are found for $N_x = 5$ network. The presence of a wide minimum, near the 2.6% level, is noteworthy for this system between 90 and 200 epochs. The screening of larger networks, $N_x = 6$–7, suggests that a large separation of neurons, which are occupied by calibrating samples in the top map, results in a poorer classification of validating samples. For example, the 7×7 network has more than 60% of all neurons empty. It seems that the

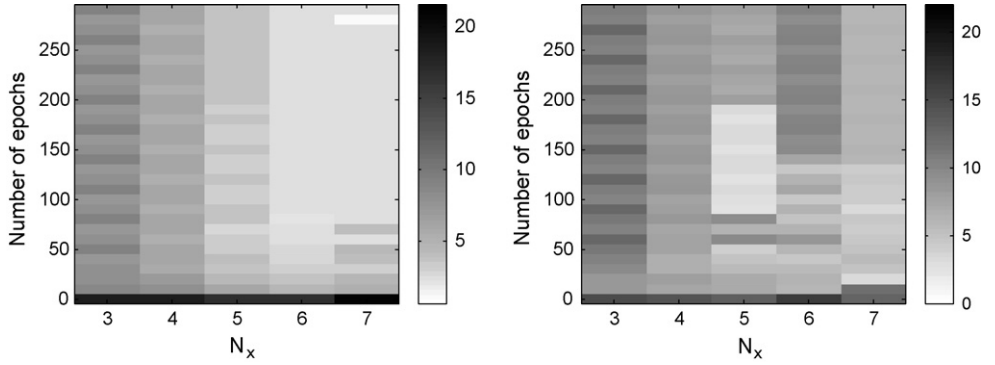

Fig. 4. Results of the screening procedure for tablets A: RSEP (%) errors for the calibration (left) and validation (right) data sets as a function of the number of neurons in the x- and y-directions and the number of learning cycles.

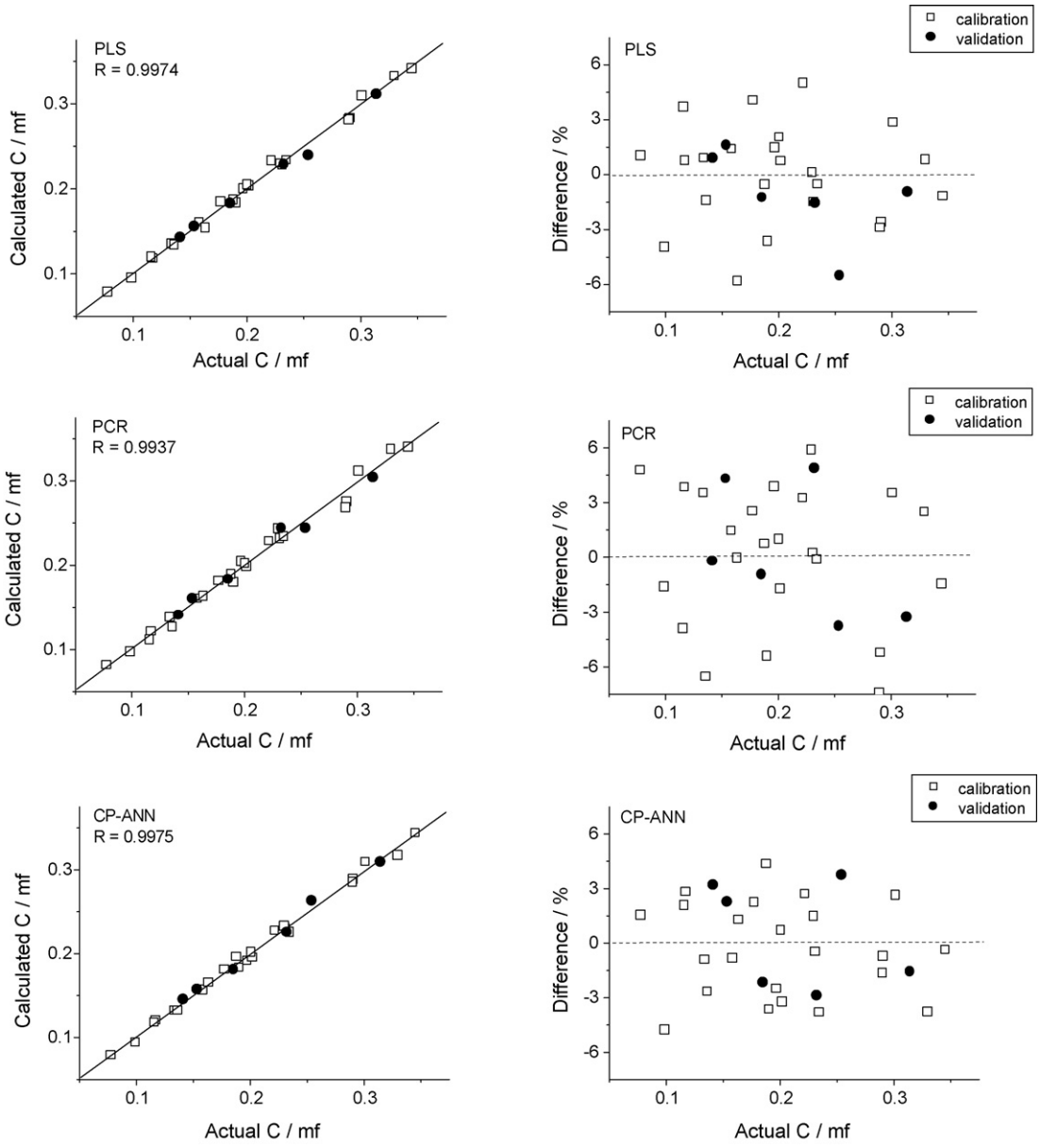

Fig. 5. Calibration curves and relative errors for the diclofenac sodium content obtained using the PLS, PCR and CP-ANN models based on unnormalised spectra.

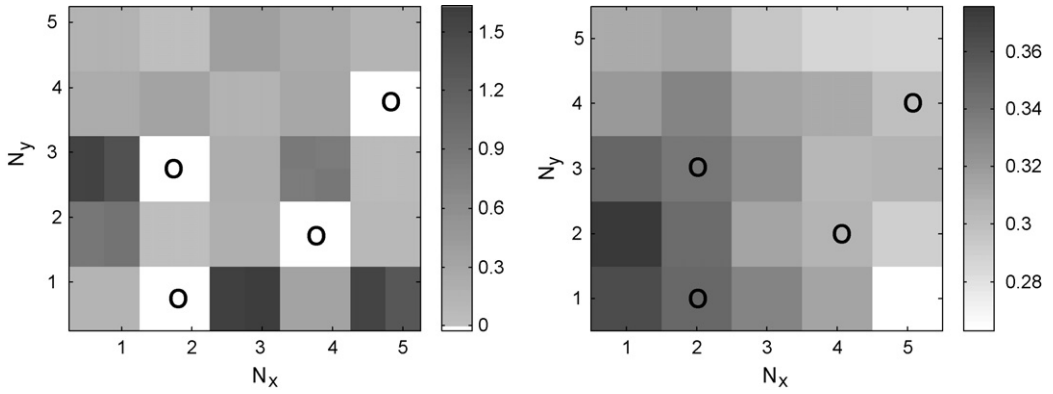

Fig. 6. CP-ANN networking for capsules E: the top map of the predicted diclofenac sodium concentrations (left), in mass fraction units, and the top map of relative accuracy (%) for the training data set (right); O—empty neurons.

Table 1
Calibration parameters for diclofenac sodium determination in tablets A

Method	Normalisation	R	$RSEP_{cal}$ (%)	$RSEP_{val}$ (%)	R_{cv}
PLS	None	0.997	2.44	2.80	0.987
	I_{max}[a]	0.996	3.05	4.85	0.985
	I_{integr}[b]	0.997	2.81	3.95	0.979
PCR	None	0.994	3.77	3.54	0.985
	I_{max}	0.993	4.06	4.38	0.991
	I_{integr}	0.993	3.97	4.28	0.991
CP-ANN	None	0.998	2.45	2.60	0.980
	I_{max}	0.995	3.32	3.78	0.982
	I_{integr}	0.994	3.64	3.49	0.987

Spectra normalised by the intensity at maximum (a) and integral intensity (b) of the internal standard band.

Table 2
Calibration parameters for diclofenac sodium determination in capsules

Model	PLS				PCR	CP-ANN
Parameter	UN	MSC	SNV	MVN		
R	0.995	0.993	0.993	0.995	0.976	0.996
$RSEP_{cal}$ (%)	0.96	1.02	1.01	0.92	1.89	0.83
$RSEP_{val}$ (%)	1.40	1.34	1.64	1.08	1.75	1.57
R_{cv}	0.947	0.949	0.920	0.943	0.942	0.944

5×5 network is optimal for the tablets and capsules studied herein. For all the analysed tablets, the minimal value of the $RSEP_{val}$ was observed between 100 and 200 learning cycles. In the case of studied capsules the lowest value of $RSEP_{val}$ error was already attained at 75 epochs.

3.1.2. Quality of the models

Typical calibration curves and plots of relative errors for the three chemometrics models applied are shown in Fig. 5. The top map of the predicted active compound concentrations as well as the top map of the relative errors of calibration for the CP-ANN modelling of preparation *E*, is presented in Fig. 6. The RSEP values found for the calibration and validation samples using the PLS, PCR and CP-ANN methods are quoted in Tables 1 and 2.

It is apparent from these data that the quality of models constructed on the basis of the PLS and CP-ANN methods are comparable, and that they both manage to effectively model the concentration-dependent changes in spectral data. The RSEP error for diclofenac sodium determination in tablet A is 2.4% for the PLS and CP-ANN models for the calibration data set. The error found from the PCR analysis is higher, at 3.8%. In the case of the analysed diclofenac sodium capsules, the difference is even more evident. The reported errors are 0.8%, 1.0% and 1.9% for the CP-ANN, PLS and PCR techniques, respectively. The external validation of models gives the $RSEP_{val}$ errors in the ranges of 2.6–3.5% for the analysed tablets and 1.4–1.8% for the capsules. However, when analysing the additives present in the studied preparations (data not listed in tables), the RSEP errors change to 2.1% for lactose and 5.4% for magnesium stearate in the diclofenac sodium tablets. In spite of the differences in the predictive ability, all three chemometrics models are characterised by a comparable resistance to the leave-one-out procedure. The cross-validation correlation coefficient value, R_{cv}, exceeds 0.94 for capsules and 0.98 for tablets.

3.2. Commercial samples

3.2.1. Quantification based on unnormalised spectra

On the basis of the constructed models studied pharmaceuticals were quantified. The mean contents of diclofenac sodium in the analysed commercial preparations determined by FT-Raman analysis are shown in Table 3. The presented values confirm that the three computational approaches applied are comparably efficient in the API quantification.

The quality of predictions of the neural networks depends on the classification criteria and the final results depend on the appropriate assignment of the quantified samples to particular neurons in the top map. Therefore, one can obtain reliable predictions for studied samples when the training set contains mixtures whose composition reflects as close as possible the composition of the analysed ones. This can be achieved for example by increasing the number of samples in the training set.

Quantification of the analysed preparations gave diclofenac sodium content, calculated against declared values, with the recovery in the ranges of 99.5–101.3%, 99.7–102.0% and 99.9–101.2% for the PLS, PCR and CP-ANN methods, respectively, as shown in Fig. 7. The mean concentrations of API found from the Raman spectra closely agree with the results of the reference analysis quoted in Table 3.

3.2.2. Quantification based on normalised spectra

The quality of substance quantification by Raman spectroscopy depends on the knowledge of the studied system composition. If the composition of the calibration mixtures closely reflects that of the analysed samples, one could expect more reliable results, but in pharmaceuticals it is sometimes difficult to identify all of the ingredients present, especially if they constitute only a part of a percent of a studied sample mass. Analysis based on a simplified model, which does not take into account some constituents present in the studied system, usually results in an increase of quan-

Table 3
Results (in milligrams) of FT-Raman analysis of the studied preparations ($n = 6$)

Method	Normalisation	Preparation (declared content)				
		Tablet A (25 mg)	Tablet B (25 mg)	Tablet C (50 mg)	Tablet D (50 mg)	Capsule E (75 mg)
PLS	None	25.12 ± 0.21	24.95 ± 0.29	50.63 ± 0.34	50.11 ± 0.64	74.62 ± 0.92
	I_{max}	25.05 ± 0.33	25.34 ± 0.49	50.26 ± 0.44	49.99 ± 0.41	
	I_{integr}	24.80 ± 0.44	25.29 ± 0.42	50.29 ± 0.84	50.07 ± 0.48	
PCR	None	24.99 ± 0.17	25.51 ± 0.31	49.91 ± 0.38	50.77 ± 0.37	74.74 ± 0.67
	I_{max}	25.13 ± 0.61	25.03 ± 0.51	50.64 ± 0.84	49.52 ± 0.73	
	I_{integr}	24.86 ± 0.53	24.96 ± 0.41	50.23 ± 0.83	50.06 ± 0.44	
CP-ANN	None	25.27[a] (100)[b]	25.28[a] (150)	50.61[a] (150)	49.94[a] (100)	75.28[a] (75)
	I_{max}	25.16 ± 0.22 (150)	25.08 ± 0.11[a] (200)	50.61 ± 0.05[a] (150)	50.24 ± 0.53 (125)	
	I_{integr}	25.54 ± 0.68 (100)	24.89 ± 0.11[a] (200)	49.47 ± 0.53 (150)	49.66 ± 0.52 (150)	
UV–vis		25.00 ± 0.32	25.10 ± 0.28	49.11 ± 0.74	50.04 ± 1.15	75.61 ± 0.62

[a] All quantified samples assigned to the same neuron, the standard deviation value is equal zero.
[b] In parenthesis the number of learning epochs used for the CP-ANN training is quoted.

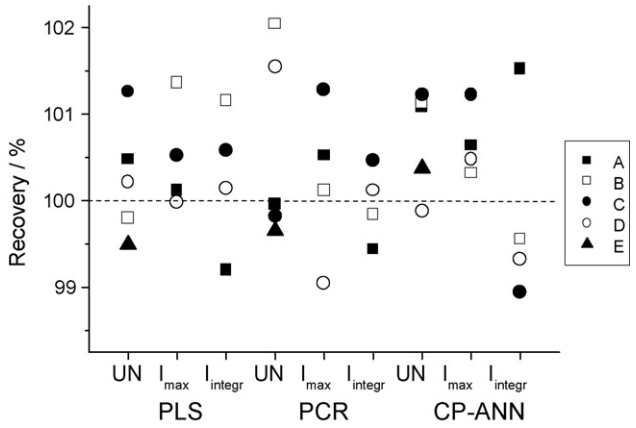

Fig. 7. Recovery of diclofenac sodium as percentages (%, w/w) of the declared amount for the studied pharmaceuticals and different analytical models.

tification errors [25,32,35]. Additional factors that can decrease the quality of quantification are connected with the incident laser beam instability and geometry changes of the incident and scattered beam during the measurements. In such cases, an internal standard method could give more reliable results. This is especially important if elaborated models were used over many weeks in a quality control setting. In light of this, potassium ferrocyanide was added as an internal standard to the mixtures modelling tablets, and Raman spectra were recorded again. New PLS, PCR and CP-ANN models were built using the spectra normalised by the intensity at the maximum and the integrated intensity of the 2091 cm^{-1} ferrocyanide line. The optimisation of spectral regions and modelling parameters was also performed again.

The results, collected in Table 1, show the influence of normalising the spectra on the quality of predictions, especially on the level of the $RSEP_{val}$ values. Errors found for the validation samples are close to 4% when the two types of normalisation were used. On the other hand, no significant differences were observed in the R_{cv} values in comparison with the cross-validation results for models based on unnormalised spectra.

Applying the calibration models mentioned above, the studied pharmaceuticals with added potassium ferrocyanide were quantified again. The mean content of diclofenac sodium found is quoted in Table 3. One can notice slightly higher standard deviation values for the determined API concentrations in comparison with those obtained on the basis of unnormalised spectra, possibly due to a relatively low S/N ratio for the analysed spectra [68]. The recovery was 99.2–101.4% for PLS, 99.0–101.3% for PCR and 98.9–101.5% for CP-ANN methods, based on normalised spectra (Fig. 7).

In addition to internal and external standard methods, there are also other possibilities for improving the quality of analysis. The most well-known are the standard normal variate (SNV) normalisation of spectra [69] and multiplicative signal correction (MSC) [70]. These methods were used during the capsule's analysis. Registered spectra were SNV-normalised or MSC-corrected and new PLS models were constructed. We also decided to apply another transformation of the spectra, i.e. their normalisation by mean intensity, calculated over the entire spectrum (MVN). This simple pretreatment procedure reduced quantification errors more efficiently than the SNV and MSC methods in the course of the hydrocarbon mixture multivariate analysis based on multiplicatively distorted FT-Raman spectral data [71].

The results presented in Table 2 indicate that only the MVN transformation of the spectra resulted in an improvement of the PLS model parameters, whereas the MSC procedure did not effect these parameters. The SNV normalised values are even worse than those obtained for the model based on untreated spectra. The quantification of diclofenac sodium in preparation E using these models gave 74.97 ± 0.88, 74.85 ± 0.66 and 74.72 ± 1.24 mg of API per capsule for the MVN, MSC and SNV methods, respectively, which were slightly better for the first two pretreatment procedures than the reference model based on the original spectra.

4. Conclusions

Five commercial preparations of diclofenac sodium, four in the form of tablets and one in capsular form, containing 25, 50 or 75 mg of API were successfully quantified using the PLS, PCR and CP-ANN models based on FT-Raman spectra. Concentrations found from the Raman data analysis agree favourably with the results of the reference analyses. They also correlate strongly with the declared values with the recovery in the 99–102% range for the different models. The proposed procedure could be a fast and convenient alternative to the standard pharmacopoeial procedures of diclofenac sodium quantification in solid dosage forms.

Acknowledgments

The authors would like to thank Röhm Pharma Polymers for the donation of the Eudragit samples and Ms. J. Romanowska for technical assistance during the initial part of this project.

References

[1] British Pharmacopoeia, HM Stationery Office, London, 1999.
[2] H. Fabre, S.W. Sun, B. Mandrou, H. Maillols, Analyst 118 (1993) 1061–1064.
[3] J.C. Botello, G. Pérez-Caballero, Talanta 42 (1995) 105–108.
[4] M.S. Garcia, M.I. Albero, C. Sánches-Pedreño, J. Molina, J. Pharm. Biomed. Anal. 17 (1998) 267–273.
[5] Y.C. de Micalizzi, N.B. Pappano, N.B. Debattista, Talanta 47 (1998) 525–530.
[6] M.L.F. de Córdova, P.O. Barrales, A.M. Díaz, Anal. Chim. Acta 369 (1998) 263–268.
[7] M.M. Sena, Z.F. Chaudhry, C.H. Collins, R.J. Poppi, J. Pharm. Biomed. Anal. 36 (2004) 743–749.
[8] P.M. Castellano, S.E. Vignaduzzo, R.M. Maggio, T.S. Kaufman, Anal. Bioanal. Chem. 382 (2005) 1711–1714.
[9] L.A. Carreira, M. Rizk, Y. El-Shabrawy, N.A. Zakhari, S.S. Toubar, J. Pharm. Biomed. Anal. 13 (1995) 1331–1337.
[10] P.C. Damiani, M. Bearzotti, M.A. Cabezón, A.C. Olivieri, J. Pharm. Biomed. Anal. 20 (1999) 587–590.
[11] J.A. Arancibia, M.A. Boldrini, G.M. Escandar, Talanta 52 (2000) 261–268.
[12] S.T. Patil, M. Sundaresan, I.C. Bhoir, A.M. Bhagwat, Talanta 47 (1998) 3–10.
[13] L. González, G. Yuln, M.G. Volonté, J. Pharm. Biomed. Anal. 20 (1999) 487–492.
[14] J. Klimeš, J. Sochor, P. Doležal, J. Körner, Int. J. Pharm. 217 (2001) 153–160.
[15] M.E. Abdel-Hamid, L. Novotny, H. Hamza, J. Pharm. Biomed. Anal. 24 (2001) 587–594.
[16] R. Hájková, P. Solich, M. Pospišilová, J. Šicha, Anal. Chim. Acta 467 (2002) 91–96.
[17] B.X. Mayer, K. Namiranian, P. Dehghanyar, R. Stroh, H. Mascher, M. Müller, J. Pharm. Biomed. Anal. 33 (2003) 745–754.
[18] A. Chmielewska, L. Konieczna, A. Plenis, H. Lamparczyk, J. Chromatogr. B 839 (2006) 102–111.
[19] C. Nebot, S.W. Gibb, K.G. Boyd, Anal. Chim. Acta 598 (2007) 87–94.
[20] A. Panusa, G. Multari, G. Incarnato, L. Gagliardi, J. Pharm. Biomed. Anal. 43 (2007) 1221–1227.
[21] O. Çakirer, E. Kiliç, O. Atakol, A. Kenar, J. Pharm. Biomed. Anal. 20 (1999) 19–26.
[22] A.M. Pimenta, A.N. Araújo, M.C.B.S.M. Montenegro, Anal. Chim. Acta 470 (2002) 185–194.
[23] M. Shamsipur, F. Jalali, S. Ershad, J. Pharm. Biomed. Anal. 37 (2005) 943–947.
[24] S.S.M. Hassan, W.H. Mahmoud, M.A.F. Elmosallamy, M.H. Almarzooqui, J. Pharm. Biomed. Anal. 39 (2005) 315–321.
[25] S. Mazurek, R. Szostak, J. Pharm. Biomed. Anal. 40 (2006) 1235–1242.
[26] T. Vankeirsbilck, A. Vercauteren, W. Baeyens, G. Van der Weken, F. Verpoort, G. Vergote, J.P. Remon, Trends Anal. Chem. 21 (2002) 869–877.
[27] M.J. Pelletier, Appl. Spectrosc. 57 (2003) 20A–42A, and references therein.
[28] P. Matousek, A.W. Parker, Appl. Spectrosc. 60 (2006) 1353–1357.
[29] C.J. Strachan, T. Rades, K.C. Gordon, J. Rantanen, J. Pharm. Pharmacol. 59 (2007) 179–192, and references therein.
[30] T.H. King, C.K. Mann, T.J. Vickers, J. Pharm. Sci. 74 (1985) 443–447.
[31] S.G. Skoulika, C.A. Georgiou, Appl. Spectrosc. 55 (2001) 1259–1265.
[32] R. Szostak, S. Mazurek, Analyst 127 (2002) 144–148.
[33] S.G. Skoulika, C.A. Georgiou, Appl. Spectrosc. 57 (2003) 407–412.
[34] A.O. Izolani, M.T. de Moraes, C.A.S. Téllez, J. Raman Spectrosc. 34 (2003) 837–843.

[35] R. Szostak, S. Mazurek, J. Mol. Struct. 704 (2004) 229–233.
[36] T.R.M. De Beer, W.R.G. Baeyens, A. Vermeire, D. Broes, J.P. Remon, C. Vervaet, Anal. Chim. Acta 589 (2007) 192–199.
[37] M. Dyrby, S.B. Engelsen, L. Nørgaard, M. Bruhn, L. Lundsberg-Nielsen, Appl. Spectrosc. 56 (2002) 579–585.
[38] S. Mazurek, R. Szostak, J. Pharm. Biomed. Anal. 40 (2006) 1225–1230.
[39] T.M. Hancewicz, C. Petty, Spectrochim. Acta A 51 (1995) 2193–2198.
[40] F. Laplant, A. De Paepe, in: S. Šašić (Ed.), Pharmaceutical Applications of Raman Spectroscopy, J. Wiley & Sons, Hoboken, 2008, pp. 85–115.
[41] B. De Spiegeleer, B. Baert, N. Diericx, D. Seghers, F. Verpoort, L. Van Vooren, C. Burvenich, G. Slegers, J. Pharm. Biomed. Anal. 44 (2007) 254–257.
[42] F. Despagne, D.L. Massart, Analyst 123 (1998) 157R–178R.
[43] S. Agatonovic-Kustrin, I.G. Tucker, D. Schmierer, Pharm. Res. 16 (1999) 1477–1482.
[44] Y. Ni, C. Liu, S. Kokot, Anal. Chim. Acta 419 (2000) 185–196.
[45] H.C. Goicoechea, M.S. Collado, M.L. Satuf, A.C. Oliveri, Anal. Bioanal. Chem. 374 (2002) 460–465.
[46] K. Kipouros, K. Kachrimanis, I. Nikolakakis, V. Tserki, S. Malamataris, J. Pharm. Sci. 95 (2006) 2419–2431.
[47] Y. Dou, N. Qu, B. Wang, Y.Z. Chi, Y.L. Ren, Eur. J. Pharm. Sci. 32 (2007) 193–199.
[48] P. Chalus, S. Walter, M. Ulmschneider, Anal. Chim. Acta 591 (2007) 219–224.
[49] H. Yang, I.R. Lewis, P.R. Griffiths, Spectrochim. Acta A 55 (1999) 2783–2791.
[50] B.K. Lavine, C.E. Davidson, D.J. Westover, J. Chem. Inf. Comput. Sci. 44 (2004) 1056–1064.
[51] K. Hennessy, M.G. Madden, J. Conroy, A.G. Ryder, Knowl.-Based Syst. 18 (2005) 217–224.
[52] V.O. Santos, F.C.C. Oliveira, D.G. Lima, A.C. Petry, E. Garcia, P.A.Z. Suarez, J.C. Rubim, Anal. Chim. Acta 547 (2005) 188–196.
[53] The European Pharmacopoeia, sixth ed., Council of Europe, Strasbourg, 2007.
[54] T. Næs, T. Isaksson, T. Fearn, T. Davies, Multivariate Calibration and Classification, NIR Publications, Chichester, 2002.
[55] H. Martens, T. Næs, Multivariate Calibration, Wiley, Chichester, 1989.
[56] F. Estienne, D.L. Massart, Anal. Chim. Acta 450 (2001) 123–129.
[57] PLS Toolbox Version 3.0, Eigenvector Research Inc., Manson, 2003.
[58] S. Wold, M. Sjöström, L. Eriksson, Chemom. Intell. Lab. Syst. 58 (2001) 109–130.
[59] M.P. Fuller, G.L. Ritter, C.S. Draper, Appl. Spectrosc. 42 (1988) 217–227.
[60] F. Estienne, D.L. Massart, N. Zanier-Szydlowski, P. Marteau, Anal. Chim. Acta 424 (2000) 185–201.
[61] J.B. Cooper, Chemom. Intel. Lab. Syst. 46 (1999) 231–247.
[62] J. Gabrielsson, N. Lindberg, T. Lundstedt, J. Chemom. 16 (2002) 141–160.
[63] J. Zupan, M. Novič, J. Gasteiger, Chemom. Intel. Lab. Syst. 27 (1995) 175–187.
[64] J. Zupan, M. Novič, I. Ruisánchez, Chemom. Intel. Lab. Syst. 38 (1997) 1–23.
[65] J. Zupan, J. Gasteiger, Neural Networks in Chemistry and Drug Design, Wiley-VCH, Weinheim, 1999.
[66] I. Kuzmanovski, M. Novič, Chemom. Intel. Lab. Syst. 90 (2008) 84–91.
[67] M. Otto, W. Wegscheider, Anal. Chem. 57 (1985) 63–69.
[68] R. Szostak, S. Mazurek, J. Mol. Struct. 704 (2004) 235–245.
[69] R.J. Barnes, M.S. Dhanoa, S.J. Lister, Appl. Spectrosc. 43 (1989) 772–777.
[70] H. Martens, E. Stark, J. Pharm. Biomed. Anal. 9 (1991) 625–635.
[71] R. Szostak, S. Mazurek, unpublished results.